European Journal of Medicinal Chemistry 80 (2014) 101–111

Contents lists available at ScienceDirect

European Journal of Medicinal Chemistry

journal homepage: http://www.elsevier.com/locate/ejmech

Original article

New indolylarylsulfones as highly potent and broad spectrum HIV-1 non-nucleoside reverse transcriptase inhibitors

Valeria Famiglini [a], Giuseppe La Regina [a,*], Antonio Coluccia [a], Sveva Pelliccia [a], Andrea Brancale [b], Giovanni Maga [c], Emmanuele Crespan [c], Roger Badia [d], Bonaventura Clotet [d], José A. Esté [d], Roberto Cirilli [e], Ettore Novellino [f], Romano Silvestri [a]

[a] Istituto Pasteur – Fondazione Cenci Bolognetti, Dipartimento di Chimica e Tecnologie del Farmaco, Sapienza Università di Roma, Piazzale Aldo Moro 5, I-00185 Roma, Italy
[b] Welsh School of Pharmacy, Cardiff University, King Edward VII Avenue, Cardiff CF10 3NB, UK
[c] Institute of Molecular Genetics IGM-CNR, National Research Council, via Abbiategrasso 207, I-27100 Pavia, Italy
[d] AIDS Research Institute – IrsiCaixa, Hospitals Germans Trias i Pujol, Universitat Autonóma de Barcelona, 08916 Badalona, Spain
[e] Istituto Superiore di Sanità, Dipartimento del Farmaco, Viale Regina Elena 299, I-00161 Roma, Italy
[f] Dipartimento di Farmacia, Università di Napoli Federico II, Via Domenico Montesano 49, I-80131, Napoli, Italy

ARTICLE INFO

Article history:
Received 22 November 2013
Received in revised form
4 March 2014
Accepted 7 April 2014
Available online 12 April 2014

Keywords:
AIDS
HIV-1
Reverse transcriptase
Nonnucleoside inhibitor
Indolylarylsulfone

ABSTRACT

New indolylarylsulfone HIV-1 NNRTIs were synthesized to evaluate unexplored substitutions of the benzyl/phenylethyl group linked at the indole-2-carboxamide. Against the NL4-3 HIV-1 WT strain, 17 out 20 compounds were superior to NVP and EFV. Several compounds inhibited the K103N HIV-1 mutant strain at nanomolar concentration and were superior to EFV. Some derivatives were superior to EFV against the Y181C and L100I HIV-1 mutant strains. Against the NL4-3 HIV-1 strain, the enantiomers **24** and **25** showed small differences of activity. In contrast, **24** turned out significantly more potent than **25** against the whole panel of mutant HIV-1 strains. The docking studies suggested that the difference in the observed inhibitory activities of **24** and **25** against the K03N mutation could be due to a kinetic rather than affinity differences.

1. Introduction

The clinical management of human immunodeficiency virus type 1 (HIV-1) infection and acquired immunodeficiency syndrome (AIDS) is based on antiretroviral agents [1], while an effective HIV-1 vaccine remains elusive [2]. HIV/AIDS agents may be viewed as falling into six drug classes: nucleoside (NRTIs) and nucleotide reverse transcriptase inhibitors (NtRTIs), non-nucleoside reverse transcriptase inhibitors (NNRTIs), protease inhibitors (PIs), fusion inhibitors (FIs), entry inhibitors – CCR5 co-receptor antagonists, and HIV integrase strand transfer inhibitors (INSTIs). These agents may be formulated either as single drug or multi-drug combination products [3]. The main treatment available for HIV/AIDS is highly active antiretroviral therapy (HAART), that includes two or three (preferably) antiretroviral drugs from different drug classes. Effective HAART regimens reduce HIV-associated morbidity and mortality maintaining plasma viremia below the detection level in most patients undergoing treatment for at least six months [4].

First-generation NNRTIs Nevirapine (NVP), Delavirdine (DLV) or Efavirenz (EFV) may lead to rapid development of drug resistance; in particular, the K103N and Y181C are the most prevalent mutations, in clinical HIV-1 isolates [5]. Etravirine (ETV) and Rilpivirine (RPV) were approved for use in drug combination to manage treatment-experienced HIV-1 infected people, and naïve and adult patients, respectively [6]. Despite their effectiveness, the viral resistance associated to NNRTI drugs and adverse effects continue to emerge in chronic long-term treatments [7]. In fact there is a pressing need for new antiretroviral agents.

In the past decade, we have developed indolylarylsulfone (IAS) HIV-1 NNRTIs [8]. Introduction of two methyl groups at positions 3′ and 5′ of the 3-phenylsulfonyl moiety led to IAS derivatives with broader spectrum of activity against mutant HIV-1 strains [9]. The space surrounding the 2-carboxamide proved to tolerate a wide variety of substituents (natural or unnatural amino acids, hydroxyethyl moiety, Mannich bases) remarkably enhancing potency of IAS analogues [10–13] (Chart 1).

* Corresponding author.
E-mail addresses: giuseppe.laregina@uniroma1.it (G. La Regina), romano.silvestri@icloud.com (R. Silvestri).

http://dx.doi.org/10.1016/j.ejmech.2014.04.027
0223-5234/

The anti-HIV-1 activity of first as well as second generation NNRTIs is hampered by the emergence of NNBS RT mutations. Recent literature reported that the introduction of an additional aromatic moiety to the parent compound resulted in NNRTIs with broad spectrum of activity against the mutant HIV-1 strains [14]. At the state of the art, only ETV is able to fit well into the NNBS despite the plasticity of mutated RTs thanks to peculiar binding mode (horseshoe shape). From docking experiments carried out in the K103N, L100I, Y181C and Y188L mutated RTs, we observed that IAS NNRTIs do not adopt the aforementioned horseshoe binding conformation, but may be considered hybrids between the two wings and horseshoe conformation [14].

Therefore, we focused on the design of inhibitors that would address this drug design strategy. SAR studies of the pendant (third) ring at the indole-2-carboxamide was not exhaustively explored, although two IASs bearing the benzyl or phenylethyl group showed high antiretroviral activity with IC_{50} values in the nanomolar range of concentration [15]. We observed that some substitutions could mimic the hydroxy group or the carboxamide function of IASs **2** or **3**, respectively. On the basis of these observations, the current study focused on designing of unexplored substitutions of the benzyl/phenylethyl group linked at the carboxamide nitrogen at position 2 of the indole. We describe the synthesis and antiretroviral activity of new IAS derivatives **4**–**23** bearing different substituents of the benzyl/phenylethyl nucleus at the indole-2-carboxamide (Table 1).

2. Chemistry

2.1. Synthetic procedures

Carboxamides **4**–**11** and **13**–**23** were synthesized by coupling reaction of 5-chloro-3-((3,5-dimethylphenyl)sulfonyl)-1*H*-indole-2-carboxylic acid (**26**) [9,10] with the appropriate amine in the presence of (benzotriazol-1-yloxy)tris(dimethylamino)-phosphonium hexafluorophosphate (BOP reagent) and triethylamine in anhydrous DMF at 25 °C for 12 h. Tin(II) chloride reduction of the nitro derivative **11** by heating at 80 °C for 3 h in ethyl acetate furnished compound **12** (Scheme 1).

(4-Dimethylaminophenyl)methanamine trifluoroacetate (**31**) was achieved by treatment of 4-nitrobenzylamine hydrochloride (**27**) with di-*tert*-butyl dicarbonate in anhydrous dichloromethane and then with triethylamine to furnish *tert*-butyl *N*-((4-nitrophenyl)methyl)carbamate (**28**). Compound **28** was reduced to amino **29** with hydrogen at 35 PSI in the presence of Pd/C as a catalyst at room temperature for 2 h. Compound **29** was transformed into the corresponding dimethyl derivative **30** by reaction with dimethylsulfate for 16 h in anhydrous acetone. The subsequent treatment of **30** with trifluoroacetic acid in anhydrous dichloromethane provided salt **31** (Scheme 2).

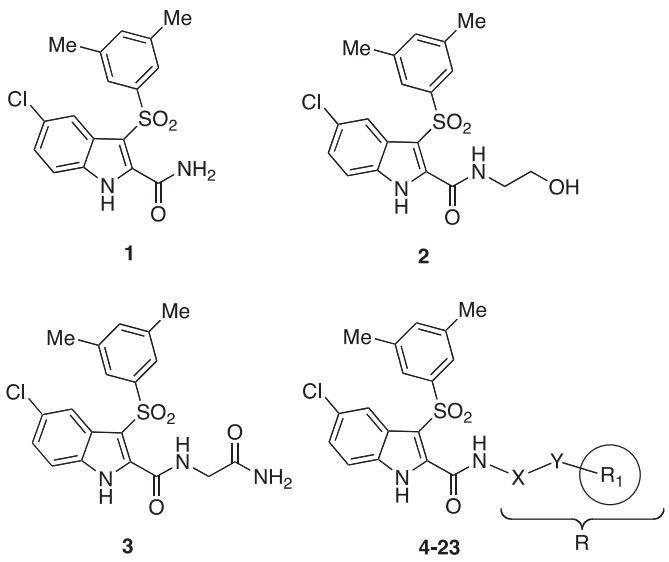

Chart 1. Structures of IAS compounds **1**–**23**.

2.2. Separation and absolute configuration assignment of the enantiomers

The direct enantioseparation of the racemate **14** was accomplished by HPLC on the cellulose derived coated Chiralcel OD chiral stationary phase (CSP) using the binary mixture *n*-hexane-ethanol 1:1 as a mobile phase (Chart 2). The optimized analytical enantioselective method was easily scaled-up to a semipreparative level. The absolute configuration assignment was carried out by a two-step strategy. In the first step, the (*S*)-enantiomer **25** was synthesized starting from the amine of known stereochemistry (*S*)-(−)-α-methylbenzylamine. In the second step, the stereochemical course of reactions was monitored by enantioselective HPLC. The elution time of (*S*)-**25** was then compared with the enantiomeric peaks of the racemate **14** under the same enantioselective HPLC conditions (Chart 2). On the Chiralcel OD CSP, the (*R*)-enantiomer **24** was eluted before the (*S*)-enantiomer **25**. The circular dichroism (CD) spectra of (*R*)-**24** and (*S*)-**25** are shown in Chart 3.

3. Results and discussion

3.1. Inhibition of HIV-1 acutely infected cells

Of the desired structural changes, we initially synthesized new IAS benzyl derivatives **4**–**15** (Table 1). Against the NL4-3 HIV-1 WT strain, compounds **4**–**15** were all superior to reference drugs NVP and EFV. Independently on nature and position of the substituent, derivatives **4**–**15** inhibited the NL4-3 strain by fifty-percent (EC_{50} values) in the low-nanomolar (**4**, **9** and **11**) or sub-nanomolar (**5**, **7**, **8**, **10**, **12** and **14**) range of concentrations (MTT method); the latter group of inhibitors were comparable to the parent unsubstituted benzyl derivative [15]. Introduction of a fluoro atom the *N*-benzyl group provided compounds **7**–**9** that potently inhibited the NL4−3 HIV-1 strain (**7**, **8**: EC_{50} = 0.68 nM; **9**: EC_{50} = 1.1 nM). On the other hand, introduction of 4-methoxy or 2-nitro group at the benzyl moiety also provided sub-nanomolar inhibitors of the NL4-3 strain (**5**: EC_{50} = 0.21 nM; **10**: EC_{50} = 0.8 nM). The replacement of the phenylethyl group with the isomeric 1-phenylethyl moiety gave **14** (EC_{50} = 0.26 nM) that was more potent than the parent compound. When tested for their cytotoxicity, **4**–**11** and **13**–**15** showed CC_{50} values >20,000 nM and selectivity indexes (SI = CC_{50}/EC_{50} ratio) which were higher than those of NVP and EVF.

The introduction of substituents at the phenylethyl moiety led to NL4-3 inhibitors active in the low nanomolar range, except those bearing the substituent at the position 4 (compare **16** and **17** (EC_{50} = 4.0 nM) with **18**, and **21** and **22** (EC_{50} = 6.2 nM) with **23**) suggesting the unfavorable steric effects of this position. As inhibitor of the NL4-3 HIV-1 strain, the 2-phenylpropyl derivative **20** was slightly more potent than the inferior homologue **14**; in contrast, the isomeric derivative **19** inhibited the IIIB HIV-1 strain at higher concentration.

IAS derivatives **4**–**23** were evaluated in MT4 cells against mutant HIV-1 strains harboring K130N, Y181C, Y188L, L100I and Y181C–K103N single or double amino acid mutations in the RT (Table 2). Derivatives **5**, **7**–**10**, **12**, **14**, **16** and **20** inhibited the mutant

Table 1
Structure and Anti-HIV activity of new IAS derivatives **4**–**23**.[a]

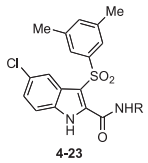

4-23

Compd	*R*	CC_{50}[b] (nM)	EC_{50} ± SD (nM) HIV-1 NL4-3[c]	SI[d]	EC_{50} ± SD (nM) HIV-1 IIIB[e]	EC_{50} (nM) HIV-2 ROD[f]
4	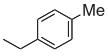	21221 ± 2077	2.1 ± 0.6	10,105	nd[g]	nd
5	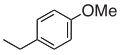	39,877 ± 13,603	0.21[h]	189,890	nd	nd
6	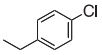	>51,293	8.2 ± 6.2	>6255	nd	nd
7		>53,085	0.68[h]	>78,066	3.6 ± 2.2	>2000[i]
8		>53,085	0.68[h]	>78,066	4.3 ± 2.3	>10000[i]
9		>53,085	1.1 ± 0.5	>48,259	5.3 ± 0.49	>10000[i]
10		>50,205	0.8 ± 0.4	>62,757	nd	nd
11	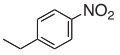	>50,205	2.0 ± 0.60	>25,106	nd	nd
12	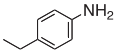	6368 ± 919	0.21[h]	8969	nd	nd
13	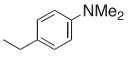	40,664 ± 6877	12.1 ± 8.1	3361	nd	nd
14[j]		>53,535	0.6[h]	>205,903	16 ± 12	>10000[i]
15	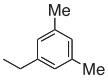	>51,974	4.2 ± 2.6	>12,375	28 ± 0.71	>2000[i]
16		44,972 ± 12,055	4.0 ± 3.1	11,243	9.4 ± 2.3	>10,000
17	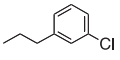	29,097 ± 8145	4.0 ± 2.9	7274	11 ± 0	>10,000
18	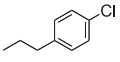	32,368 ± 9206	53.8 ± 32.4	602	68 ± 46	>10,000
19[j]		nd	nd	nd	91 ± 9	nd
20[j]		19,937 ± 5223	0.21[h]	94,938	nd	nd
21		>51,974	6.2 ± 3.0	8383	9.1 ± 2.7	>10,000

(*continued on next page*)

Table 1 (*continued*)

Compd	*R*	CC_{50}[b] (nM)	EC_{50} ± SD (nM) HIV-1 NL4-3[c]	SI[d]	EC_{50} ± SD (nM) HIV-1 IIIB[e]	EC_{50} (nM) HIV-2 ROD[f]
22	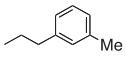	>51,974	6.2 ± 3.4	8383	7.3 ± 0.71	>25,000
23	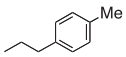	>51,974	22.9 ± 14.8	2270	33 ± 4.2	>50,000
NVP	–	>18,776	112.4 ± 74.9	>167	19.2 ± 0.0	>10,000
EFV	–	>15,839	15.9 ± 12.7	>996	1.5 ± 0.3	>10,000
AZT	.	>30,595	3.7 ± 3.7	>8269	nd	nd

[a] Data are mean values of two to three independent experiments each one in triplicate.
[b] CC_{50}: cytotoxic concentration (nM) to induce 50% death of non-infected cells, as evaluated with the MTT method in MT-4 cells.
[c] EC_{50} (HIV-1 NL4-3): effective concentration (nM) to inhibit by 50% HIV-1 (NL4–3 strain) induced cell death, as evaluated with the MTT method in MT-4 cells.
[d] SI: selectivity index calculated as CC_{50}/EC_{50} ratio.
[e] EC_{50} (HIV-1 III_B): effective concentration (nM) or concentration required to protect CEM cells against the cytopathicity of HIV-1 (III_B strain) by 50%, as monitored by giant cell formation.
[f] EC_{50} (HIV-2 ROD): effective concentration (nM) or concentration required to protect CEM cells against the cytopathicity of HIV-2 (ROD strain) by 50%, as monitored by giant cell formation.
[g] nd: no data.
[h] Lowest detectable nM concentration.
[i] Compound precipitation was detected at higher compound concentration.
[j] Data of D,L racemic mixture.

K103N HIV-1 strain in the nanomolar range with EC_{50}s ranging from 4.2 nM (**12**) to 37 nM (**16**). Such compounds were significantly superior to EFV. The most potent inhibitors **8** and **12** were >546-fold and >3-fold more potent than EFV and AZT, respectively. Against the Y181C mutant strain, five compounds, namely **5**, **8** and **10**–**12** were superior to EFV. Against this mutant strain, the most potent derivative **8** (EC_{50} = 4.3 nM) went 37-fold higher than EFV and at the same level of AZT. Compounds **10** and **12** proved to be 2.7- and 1.5-fold superior to EFV as inhibitor of the Y188L HIV-1 strain.

Several new IASs inhibited the mutant L100I HIV-1 strain at nanomolar concentration, with the exception of compounds **18** and **19**. The fluoro derivative **7**–**9** ($EC_{50} \approx 5$ nM) were uniformly active against this HIV-1 mutant strain, and went about 4- and 10-fold more active than NVP and EFV. IAS derivatives **4**–**23** proved to be weak inhibitors of the double mutant K103N–Y181C HIV-1 strain, although derivatives **7**, **10**, **12** and **14** were inhibitory of this mutant strain in the micromolar range of concentration, and **12** was the most potent derivative with EC_{50} = 598 nM.

To evaluate the influence of the asymmetric center at the 1-phenylethyl moiety, the racemic mixture **14** was separated using a chiral HPLC to give the pure enantiomers **24** and **25** (Table 3). Against the NL4-3 HIV-1 strain, the enantiomers **24** and **25** showed small differences of activity. In contrast, **24** turned out significantly more potent than **25** against the whole panel of mutant HIV-1 strains: 30-fold *vs* the K103N, 40-fold *vs* Y181C, >189-fold *vs* Y188L, and >22-fold *vs* K103N–Y181C.

3.2. Inhibition of HIV-1 reverse transcriptase

As inhibitors of the RT of HIV-1 WT, the majority of the IAS compounds examined were superior to NVP, with the exception of derivatives **16** and **23** (IC_{50} values, Table 4). Several IASs were comparable or superior (**5**, **9**, **10** and **12**) to EFV, and compounds **5** and **12** were in the range of concentration of ETV. Eight compounds inhibited the mutant K103N RT HIV-1 at submicromolar concentration. As inhibitors of the K103N RT compounds **9**, **10** and **12** were equipotent to ETV and remarkably more potent than NVP and EFV. The K103N mutation often emerges in EFV-treated patients, who show rebounding of viral load after an initial response to this drug [16]. Compounds **7**–**9**, **14** and **17** potently inhibited the L100I RT mutant, and compound **17** proved to highly effective against this mutant at the same level of ETV. Against the Y181I RT compound **12** that was equipotent to ETV, while the other tested compounds showed to be weak inhibitors of this HIV-1 muted RT.

Against the HIV-1 RTs, the enantiomers **24** and **25** showed IC_{50} values that were in good agreement with the corresponding cellular data depicted in Table 3 (Table 5). IASs **24** and **25** were almost equipotent against the HIV-1 WT RT. As inhibitors of the HIV-1 K103N mutated RT **24** (IC_{50} = 90 nM) proved to be remarkably more potent (104-fold) than **25**. A possible explanation of these results is discussed in the molecular modeling section. Again, IAS **24** was superior to **25**, although to a less extend, against the HIV-1 Y181C, L100I and V106A mutated RTs.

3.3. Molecular modeling

We evaluated the binding mode of compounds **4**–**23** in complex with the HIV-1 WT RT and K103N mutated RT by following our previously reported methodology [15]. From the molecular docking results we observed that the proposed binding mode was consistent through the whole training set and also coherent with the one previously reported for the IAS family [8–11]. For the WT RT we highlighted some established pharmacophoric interactions: i) an H-bond between the indole NH and the carbonyl oxygen of the Lys101; ii) the steric interactions between the chlorine atom in the pocket formed by Val106 and Leu234; iii) a series of hydrophobic interactions between the 3,5-dimethylphenyl moiety in the aromatic cleft formed by Tyr181, Tyr188, and Trp229 residues; iv) the hydrophobic interactions between the substituted phenyl ring and the aliphatic linker with Val179 and Ile 180 and the side chains of Glu138:B and Thr139:B. Consistent with the proposed binding mode, compounds **15** and **23** were partly located out of the NNRTI entrance pocket and exposed to the solvent. It should be noted that the two enantiomers **24** and **25** showed a very similar binding mode (Fig. 1).

Interestingly, the molecular docking into the K103N mutated RT gave apparently similar results to the corresponding ones obtained using the WT RT. However, when the binding poses of the enantiomers **24** and **25** were carefully examined, a small, yet significant

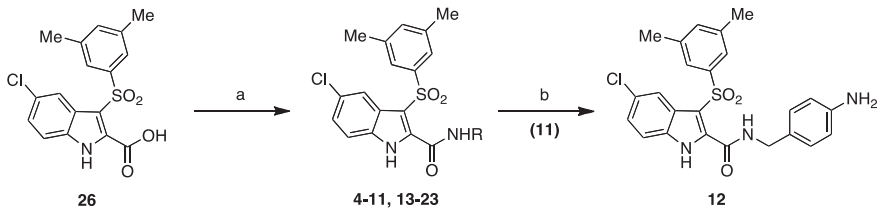

Scheme 1. Synthesis of compounds **4**–**23**. Reagents and reaction conditions: (a) amine, BOP reagent, triethylamine, anhydrous DMF, 25 °C, 12 h, 15–80%; (b) $SnCl_2 \cdot 2H_2O$, AcOEt, 80 °C, 3 h, 9%.

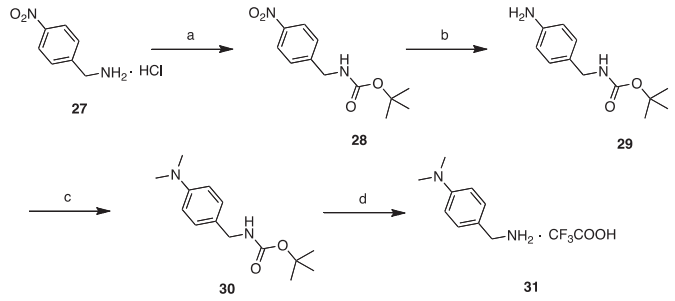

Scheme 2. Synthesis of amine **31**. Reagents and reaction conditions: (a) (i) Boc_2O, triethylamine, anhydrous CH_2Cl_2, 0 °C, 10 min; (ii) 25 °C, 2 h, 91%; (b) Pd/C, MeOH, Ar stream, 35 PSI, 2 h, 100%; (c) $(MeO)_2SO_2$, K_2CO_3, anhydrous acetone, 25 °C, 16 h, 41%; (d) TFA, CH_2Cl_2, 25 °C, 30 min 77%.

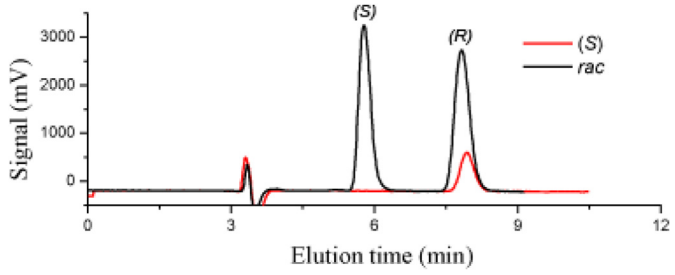

Chart 2. Chromatograms of the resolution of the racemate **14** and the (*S*)-enantiomer purity control. Column Chiralcel OD 250 mm × 4.6 mm I.D.; detection UV at 280 nm; *n*-hexane-ethanol 1:1 (v/v) as eluent; flow rate 1.0 mL min^{-1}; column temp. 25 °C.

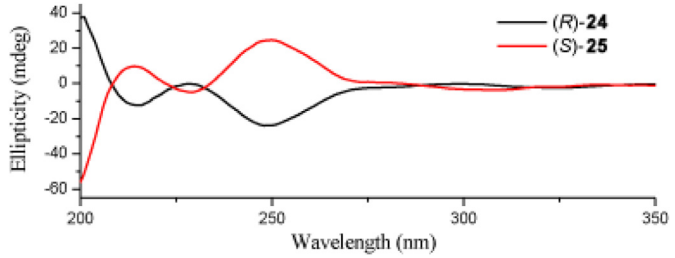

Chart 3. CD Spectra of enantiomers (*R*)-**24** and (*S*)-**25**. Solvent ethanol; temp. 20 °C.

difference was observed. The K103N mutation created a small gap at the entrance channel of the NNRTI binding site and while the methyl group of the (*R*)-enantiomer **24** pointed toward this cleft, the corresponding group of the (*S*)-enantiomer **25** pointed toward the bottom of the cleft, leaving the binding pocket more exposed to the aqueous environment (Fig. 2). It was reported that the drug resistance induced by the K103N mutation is related to a kinetic effect that affects the on/off rate of the binding of the inhibitor rather than to the breakage of binding contacts between the inhibitor and the RT [18]. The docking results obtained for **24** and **25** suggested that the difference in the observed biological activity for these compounds could be due to a different binding kinetic rather than affinity: while compound **24** was able to seal the binding pocket, **25** left the site accessible to water, leading to a negative effect on the binding kinetic of this inhibitor.

4. Conclusions

We designed and synthesized new indolylarylsulfones as HIV-1 NNRTIs in order to evaluate unexplored substitutions of the benzyl/phenylethyl group linked at the carboxamide nitrogen at position 2 of the indole. Against the NL4–3 HIV-1 WT strain, 17 out 20 compounds were superior to the references NVP and EFV. Several compounds inhibited the K103N HIV-1 mutant strain at nanomolar range of concentration and were superior to EFV, and some derivatives were superior to EFV against the Y181C and L100I HIV-1 mutant strains. Against the NL4-3 HIV-1 strain, the enantiomers **24** and **25** showed small differences of activity. In contrast, **24** turned out significantly more potent than **25** against the whole panel of mutant HIV-1 strains. The enzymatic results for **24** and **25** were in well agreement with the cellular data. The docking studies suggested that the difference in the observed inhibitory activities of **24** and **25** could be due to a kinetic rather than affinity differences. Compound **24** represents a robust lead compound to develop NNRTIs with improved activity and selectivity against K103N that is the most frequently emerging HIV-1 mutation in EFV-treated patients [16]. These results warrant further exploration of the arylalkyl moiety at the indole-2-carboxamide to obtain new IAS derivatives that have potential as novel therapeutic agents to treat AIDS/HIV-1 infection.

5. Experimental protocols

5.1. Chemistry

All reagents and solvents were commercially available and used without further purification. Organic solutions were dried over anhydrous sodium sulfate. Evaporation of the solvents was carried out on a Büchi Rotavapor R-210 equipped with a Büchi V-850 vacuum controller and Büchi V-700 (~5 mbar) and V-710 (~2 mbar) vacuum pumps. Column chromatography was run on glass columns packed with aluminum oxide 90 standardized (Merck) or silica gel (Macherey–Nagel, 63–200 μm) eluting with the indicated solvent. Aluminum oxide thin layer chromatography (TLC) cards from Fluka (aluminum oxide precoated aluminum cards with fluorescent indicator detectable at 254 nm) and silica gel TLC cards from Macherey–Nagel (silica gel precoated aluminum cards with fluorescent indicator detectable at 254 nm) were used for TLC.

Table 2
Anti-HIV-1 activity of compounds **4**–**23** against mutant HIV-1 strains.[a,b]

Compd	EC_{50} ± SD (nM)/FC[c]				
	K103N	Y181C	Y188L	L100I	K103N–Y181C
4	385 ± 6.4 183	215 ± 86 103	>21,221 >10,105	nd[d]	>21221 >10,105
5	21 ± 4.1 100	21 ± 8.4 100	>39,177 >186,557	nd	>39,177 >186,557
6	103 ± 113 13	451 ± 328 55	>51,292 >6255	nd	>51,292 >6255
7	7.8 ± 2.3 11.5	220 ± 260 324	nd[c]	5.4 ± 1.2 7.9	2144 ± SD 3153
8	4.4 ± 3.3 6.5	4.3 ± 5.7 6.3	nd	5.0 ± 0.9 7.4	13,866 ± SD 20,391
9	16 ± 15 14.5	160 ± 57 145	nd	5.9 ± 0.4 5.4	50,325 ± SD 45,750
10	6.0 ± 4.0 7.5	16 ± 14 20	281 ± 181 351	nd	1868 ± 2410 2335
11	120 ± 60 60	70 ± 80 35	>50,206 >25,103	nd	>50,206 >25,103
12	4.3 ± 2.1 20	11 ± 9.8 52	491 ± 112 2338	nd	598 ± 321 2847
13	322 ± 161 27	1028 ± 524 85	>40,321 >3332	nd	>40,321 >3332
14[e]	33 ± 6.4 55	720 ± 690 1200	nd	26 ± 24 43	3267 ± SD 5445
15	180 ± 21 43	>2000[f] >476	nd	65 ± 21 15	>51,794 >12,332
16	37 ± 28 9.3	250 ± 28 63	nd	24 ± 4.2 6.0	44,972 11,243
17	180 ± 71 45	870 ± 130 218	nd	31 ± 12 7.8	29,097 7274
18	≥2000 ≥37	1700 ± 490 36	nd	190 ± 64 3.5	32,368 602
19[e]	530 ± 110 5.8[g]	>1000 >11	>1000 >11	380 ± 340 4.2	>2079 23
20[e]	29 ± 11 138	291 ± 78 1386	>19,937 >94,938	nd	>19,937 >94,938
21	100 ± 69 16	850 ± 7.1 1371	nd	20 ± 15 3.2	>51,937 >8383
22	260 ± 210 42	1200 ± 71 194	nd	31 ± 2.8 5.0	>51,937 >8383
23	>50,000 2183	1800 ± 40 79	nd	nd	>51,937 >2268
NVP	>3756 >33	>3756 >33	>3756 >33	60 ± 4 1.8	>3756 >33
EFV	130 ± 180 8.2	160 ± 180 10	760 ± 630 48	22 ± 14 1.4	>317 >20
AZT	16 ± 12 4.3	6.0 ± 3.4 1.6	33 ± 18 8.9	nd	16 ± 13 1.0

[a] Data are mean values of two to three independent experiments each one in triplicate.
[b] EC_{50}: effective concentration (nM) to inhibit by 50% cell death induced by the indicated mutant HIV-1 strain, as evaluated with the MTT method in MT-4 cells.
[c] FC: fold change obtained as ratio between EC_{50}s of the indicated drug resistant mutant HIV-1 strain and HIV-1 WT NL4-3 strain.
[d] nd: no data.
[e] Data of D,L racemic mixture.
[f] Compound precipitation was detected at higher compound concentration.
[g] FC: fold change obtained as ratio between EC_{50}s of the indicated drug resistant mutant HIV-1 strain and HIV-1 WT IIIB strain.

Developed plates were visualized by a Spectroline ENF 260C/FE UV apparatus. Flash chromatography was carried out on Interchim Spot II Flash, using Merck SuperVarioFlash D26 cartridges packed with Merck Geduran 60 (40–63 μm) silica gel. Melting points (mp) were determined on a SMP1 apparatus (Stuart Scientific) and are uncorrected. IR spectra were run on a SpectrumOne FT-ATR spectrophotometer (Perkin Elmer). Band position and absorption ranges are given in cm^{-1}. Proton (^1H NMR) and carbon (^{13}C NMR) nuclear magnetic resonance spectra were recorded on a 400 MHz FT spectrometer (Bruker) in the indicated solvent. Chemical shifts are expressed in δ units (ppm) from tetramethylsilane. Elemental analyses of tested compounds were found within 0.4% of the theoretical values. Combustion analysis was used as a method of establishing compound purity. Purity of tested compounds was ≥95%.

*5.1.1. General procedure for the preparation of derivatives **4**–**11** and **13**–**23**. Example. 5-Chloro-3-((3,5-dimethylphenyl)sulfonyl)-N-(4-methylbenzyl)-1H-indole-2-carboxamide (**4**)*

A mixture of **26** [9,10] (100 mg, 0.27 mmol), 4-tolylmethanamine (100 mg, 0.08 mL, 0.81 mmol), BOP reagent (120 mg, 0.27 mmol), and triethylamine (80 mg, 0.11 mL, 0.81 mmol) in anhydrous DMF (5 mL) was stirred at 25 °C for 12 h. The reaction mixture was diluted with water and extracted with ethyl acetate. The organic layer was washed with brine, dried and filtered. Removal of the solvent gave a residue that was purified by column chromatography (silica gel, ethyl acetate:*n*-hexane = 1:2 as eluent) to furnish **4** (70 mg, 56%), mp 240–242 °C (from ethanol). ^1H NMR (DMSO-d_6): δ 2.26 (s, 6H), 2.29 (s, 3H), 4.53 (d, J = 6.0 Hz, 2H), 7.17 (d, J = 7.8 Hz, 2H), 7.24 (s, 1H), 7.32–7.35 (m, 3H), 7.53 (d, J = 8.9 Hz, 1H), 7.58 (s, 2H), 7.93 (d, J = 1.8 Hz, 1H), 9.39 (t, J = 5.3 Hz, 1H, disappeared on treatment with D_2O), 13.05 ppm (br s, 1H, disappeared on treatment with D_2O). IR: ν 1651, 2920, 3219 cm^{-1}. Anal. Calcd. for $C_{25}H_{23}ClN_2O_3S$: C, 64.30%; H, 4.96%, N, 6.00%; Cl, 7.59%; S, 6.87%. Found: C, 64.08%; H, 4.90%, N, 5.84%; Cl, 7.41%; S, 6.60%.

*5.1.2. 5-Chloro-3-((3,5-dimethylphenyl)sulfonyl)-N-(4-methoxybenzyl)-1H-indole-2-carboxamide (**5**)*

It was synthesized as **4** starting from **26** and (4-methoxyphenyl) methanamine. Yield 37%, mp 250–254 °C (from ethanol). ^1H NMR (DMSO-d_6): δ 2.26 (s, 6H), 3.74 (s, 3H), 4.53 (d, J = 5.7 Hz, 2H), 6.92 (d, J = 8.3 Hz, 2H), 7.24 (s, 1H), 7.32–7.37 (m, 3H), 7.52 (d, J = 8.8 Hz, 1H), 7.57 (s, 2H), 7.93 (s, 1H), 9.37 (t, J = 5.0 Hz, 1H, disappeared on treatment with D_2O), 13.05 ppm (br s, 1H, disappeared on treatment with D_2O). ^{13}C NMR (DMSO-d_6): δ 21.33, 43.08, 55.71, 112.06, 114.43, 115.53, 119.55, 124.25, 125.29, 125.92, 127.87, 129.63, 130.77, 133.54, 135.28, 137.65, 139.56, 143.14, 159.11, 159.82 ppm. IR: ν 1643, 3209 cm^{-1}. Anal. Calcd. for $C_{25}H_{23}ClN_2O_4S$: C, 62.17%; H, 4.80%, N, 5.80%; Cl, 7.34%; S, 6.64%. Found: C, 61.92%; H, 4.77%, N, 5.61%; Cl, 7.18%; S, 6.41%.

*5.1.3. 5-Chloro-N-(4-chlorobenzyl)-3-((3,5-dimethylphenyl) sulfonyl)-1H-indole-2-carboxamide (**6**)*

It was synthesized as **4** starting from **26** and (4-chlorophenyl) methanamine. Yield 74%, mp 260–265 °C (from ethanol). ^1H NMR (DMSO-d_6): δ 2.26 (s, 6H), 4.57 (d, J = 5.7 Hz, 2H), 7.24 (s, 1H), 7.33 (d, J = 8.9 Hz, 1H), 7.41–7.48 (m, 4H), 7.53 (d, J = 8.8 Hz, 1H), 7.59 (s, 2H), 7.92 (s, 1H) 9.47 (br s, 1H, disappeared on treatment with D_2O), 13.07 ppm (br s, 1H, disappeared on treatment with D_2O). IR: ν 1650, 3214 cm^{-1}. Anal. Calcd. for $C_{24}H_{20}Cl_2N_2O_3S$: C, 59.14%; H, 4.14%, N, 5.75%; Cl, 14.55%; S, 6.58%. Found: C, 58.92%; H, 4.09%, N, 5.52%; Cl, 14.38%; S, 6.42%.

*5.1.4. 5-Chloro-3-((3,5-dimethylphenyl)sulfonyl)-N-(2-fluorobenzyl)-1H-indole-2-carboxamide (**7**)*

It was synthesized as **4** starting from **26** and (2-fluorophenyl) methanamine. Yield 22%, mp 267–270 °C (from ethanol). ^1H NMR (DMSO-d_6): δ 2.28 (s, 6H), 4.63 (d, J = 5.4 Hz, 2H), 7.21–7.27 (m, 3H), 7.34–7.42 (m, 2H), 7.54–7.60 (m, 4H), 7.95 (s, 1H), 9.47 (t, J = 4.9 Hz, 1H, disappeared on treatment with D_2O), 13.11 ppm (br s, 1H, disappeared on treatment with D_2O). ^{13}C NMR (DMSO-d_6): δ 21.18, 37.23, 115.44, 115.54, 115.75, 119.35, 124.07, 124.84, 124.89, 125.04, 125.23, 125.43, 127.63, 129.73, 129.86, 130.43, 130.49, 135.08, 139.37, 143.05, 158.94, 160.07 ppm. IR: ν 1644, 3213 cm^{-1}. Anal. Calcd. for $C_{24}H_{20}ClFN_2O_3S$: C, 61.21%; H, 4.28%, N, 5.95%; Cl, 7.53%; F, 4.03%; S,

Table 3
Anti-HIV-1 activity of racemate **14** and its enantiomers **24** and **25** against mutant HIV-1 strains.[a,b]

Compd (*Chirality*)	EC_{50} ± SD (nM)/FC[c]					
	WT	K103N	Y181C	Y188L	L100I	K103N–Y181C
14[d]	0.6[e]	33 ± 6.4	720 ± 690	nd[f]	26 ± 24	3267 ± 2110
(*R*,*S*)		55	1200		43	5445
24	2.1 ± 1.9	4.3 ± 3.2	86 ± 43	193 ± 64	nd	1670 ± 1177
(*R*)		2.0	41	92		795
25	6.3 ± 4.2	128 ± 107	3469 ± 1735	>36,404	nd	>36,404
(*S*)		20	550	>5778		>5778

[a] Data are mean values of two to three independent experiments each one in triplicate.
[b] EC_{50}: effective concentration (nM) to inhibit by 50% cell death induced by the indicated mutant HIV-1 strain, as evaluated with the MTT method in MT-4 cells.
[c] FC: fold change obtained as ratio between EC_{50}s of the indicated drug resistant mutant HIV-1 strain and HIV-1 WT NL4-3 strain.
[d] Data of D,L racemic mixture.
[e] Lowest detectable nM concentration.
[f] nd: no data.

6.81%. Found: C, 60.92%; H, 4.22%, N, 5.77%; Cl, 7.29%; F, 3.83%; S, 6.65%.

5.1.5. 5-Chloro-3-((3,5-dimethylphenyl)sulfonyl)-N-(3-fluorobenzyl)-1H-indole-2-carboxamide (**8**)

It was synthesized as **4** starting from **26** and (3-fluorophenyl) methanamine. Yield 22%, mp 260–264 °C (from ethanol). ^{1}H NMR (DMSO-d_6): δ 2.28 (s, 6H), 4.62 (d, J = 5.8 Hz, 2H), 7.10–7.15 (m, 1H), 7.25–7.45 (m, 5H), 7.55 (d, J = 8.7 Hz, 1H), 7.63 (s, 2H), 7.94 (d, J = 1.7 Hz, 1H), 9.51 (t, J = 5.8 Hz, 1H, disappeared on treatment with D_2O), 13.1 ppm (br s, 1H, disappeared on treatment with D_2O). IR: ν 1649, 3206 cm^{-1}. Anal. Calcd. for $C_{24}H_{20}ClFN_2O_3S$: C, 61.21%; H, 4.28%, N, 5.95%; Cl, 7.53%; F, 4.03%; S, 6.81%. Found: C, 61.03%; H, 4.25%, N, 5.82%; Cl, 7.30%; F, 3.88%; S, 6.55%.

5.1.6. 5-Chloro-3-((3,5-dimethylphenyl)sulfonyl)-N-(4-fluorobenzyl)-1H-indole-2-carboxamide (**9**)

It was synthesized as **4** starting from **26** and (4-fluorophenyl) methanamine. Yield 22%, mp 275–277 °C (from ethanol). ^{1}H NMR (DMSO-d_6): δ 2.28 (s, 6H), 4.58 (d, J = 5.8 Hz, 2H), 7.19–7.25 (m, 3H), 7.35 (dd, J = 2.0 and 8.7 Hz, 1H), 7.48–7.56 (m, 3H), 7.61 (s, 2H), 7.94 (d, J = 2.0 Hz, 1H), 9.47 (t, J = 5.7 Hz, 1H, disappeared on treatment with D_2O), 13.1 ppm (br s, 1H, disappeared on treatment with D_2O). IR: ν 1648, 3210 cm^{-1}. Anal. Calcd. for $C_{24}H_{20}ClFN_2O_3S$: C, 61.21%; H, 4.28%, N, 5.95%; Cl, 7.53%; F, 4.03%; S, 6.81%. Found: C, 60.98%; H, 4.21%, N, 5.70%; Cl, 7.32%; F, 3.80%; S, 6.66%.

5.1.7. 5-Chloro-3-((3,5-dimethylphenyl)sulfonyl)-N-(2-nitrobenzyl)-1H-indole-2-carboxamide (**10**)

It was synthesized as **4** starting from **26** and (2-nitrophenyl) methanamine. Yield 75%, mp 180 °C dec. (from ethanol). ^{1}H NMR (DMSO-d_6): δ 2.28 (s, 6H), 4.88 (d, J = 4.7 Hz, 2H), 7.25 (s, 1H), 7.35 (d, J = 8.9 Hz, 1H), 7.54–7.59 (m, 4H), 7.75–7.83 (m, 2H), 7.94 (s, 1H), 8.12 (d, J = 7.9 Hz, 1H) 9.57 (br s, 1H, disappeared on treatment with D_2O), 13.12 ppm (br s, 1H, disappeared on treatment with D_2O). ^{13}C NMR (DMSO-d_6): δ 21.17, 112.15, 115.43, 119.37, 124.11, 125.20, 125.69, 127.73, 129.12, 130.57, 133.48, 133.53, 134.37, 135.13, 137.08, 139.40, 142.89, 148.32, 160.37 ppm. IR: ν 1644, 3214 cm^{-1}. Anal. Calcd. for $C_{24}H_{20}ClN_3O_5S$: C, 57.89%; H, 4.05%, N, 8.44%; Cl, 7.12%; S, 6.44%. Found: C, 57.63%; H, 4.00%, N, 8.29%; Cl, 6.98%; S, 6.20%.

5.1.8. 5-Chloro-3-((3,5-dimethylphenyl)sulfonyl)-N-(4-nitrobenzyl)-1H-indole-2-carboxamide (**11**)

It was synthesized as **4** starting from **26** and (4-nitrophenyl) methanamine. Yield 30%, mp 150 °C dec (from ethanol). ^{1}H NMR (DMSO-d_6): δ 2.25 (s, 6H), 4.69 (d, J = 8.1 Hz, 2H), 7.22 (s, 1H), 7.32 (d, J = 10. Hz, 1H), 7.52 (d, J = 11.9 Hz, 1H), 7.60 (s, 2H), 7.7 (d, J = 10.3 Hz, 2H), 7.9 (s, 1H), 8.21 (d, J = 10.6 Hz, 2H), 9.58 (br s, 1H, disappeared on treatment with D_2O), 11.68 ppm (br s, 1H, disappeared on treatment with D_2O). IR: ν 1647, 3225 cm^{-1}. Anal. Calcd. for $C_{24}H_{20}ClN_3O_5S$: C, 57.89%; H, 4.05%, N, 8.44%; Cl, 7.12%; S, 6.44%. Found: C, 57.65%; H, 3.97%, N, 8.32%; Cl, 6.94%; S, 6.28%.

5.1.9. 5-Chloro-N-(4-dimethylaminobenzyl)-3-((3,5-dimethylphenyl)sulfonyl)-1H-indole-2-carboxamide (**13**)

It was synthesized as **4** starting from **26** and (4-dimethylaminophenyl)methanamine trifluoroacetate (**31**). Yield 77%, mp 230 °C dec (from ethanol). ^{1}H NMR (DMSO-d_6): δ 2.25 (s, 6H), 2.87 (s, 6H), 4.45 (d, J = 5.9 Hz, 2H), 6.72 (d, J = 8.6 Hz, 2H), 7.25 (d, J = 8.8 Hz, 3H), 7.33 (d, J = 9.1 Hz, 1H), 7.51–7.55 (m, 3H), 7.94 (s, 1H), 9.3 (br s, 1H, disappeared on treatment with D_2O), 13.03 (br s, 1H, disappeared on treatment with D_2O). IR: ν 1649, 3192, 3282 cm^{-1}. Anal. Calcd. for $C_{26}H_{26}ClN_3O_3S$: C, 62.96%; H, 5.28%, N, 8.47%; Cl, 7.15%; S, 6.46%. Found: C, 62.81%; H, 5.22%, N, 8.29%; Cl, 6.96%; S, 6.28%.

5.1.10. 5-Chloro-3-((3,5-dimethylphenyl)sulfonyl)-N-(1-phenylethyl)-1H-indole-2-carboxamide (**14**)

It was synthesized as **4** starting from **26** and 1-phenylethanamine. Yield 57%, mp 193–197 °C (from ethanol). ^{1}H NMR (DMSO-d_6): δ 1.52 (d, J = 6.7 Hz, 3H), 2.27 (s, 6H), 5.19–5.22 (m, 1H), 7.25–7.39 (m, 5H), 7.47 (d, J = 7.4 Hz, 2H), 7.53 (d, J = 8.8 Hz, 1H), 7.57 (s, 2H), 7.94 (s, 1H), 9.42 (d, J = 7.8 Hz, 1H, disappeared on treatment with D_2O), 13.02 ppm (s, 1H, disappeared on treatment with D_2O). ^{13}C NMR (DMSO-d_6): δ 21.20, 22.82, 49.58, 111.77, 115.38, 119.42, 124.03, 125.20, 125.83, 126.69, 127.50, 127.76, 128.88, 133.35, 135.17, 137.47, 139.46, 143.01, 143.82, 158.81 ppm. IR: ν 1647, 3214, 3273 cm^{-1}. Anal. Calcd. for $C_{25}H_{23}ClN_2O_3S$: C, 64.30%; H, 4.96%, N, 6.00%; Cl, 7.59%; S, 6.87%. Found: C, 64.11%; H, 4.91%, N, 5.78%; Cl, 7.42%; S, 6.70%.

5.1.11. 5-Chloro-N-(3,5-dimethylbenzyl)-3-((3,5-dimethylphenyl)sulfonyl)-1H-indole-2-carboxamide (**15**)

It was synthesized as **4** starting from **26** and (3,5-dimethylphenyl)methanamine. Yield 15%, mp 256–260 °C (from ethanol). ^{1}H NMR (DMSO-d_6): δ 2.26 (s, 12H), 4.5 (d, J = 5.3 Hz, 2H), 6.91 (s, 1H), 7.05 (s, 2H), 7.24 (s, 1H), 7.33 (d, J = 9.0 Hz, 1H), 7.53 (d, J = 9.2 Hz, 1H), 7.59 (s, 2H), 7.93 (s, 1H), 9.36 (br s, 1H, disappeared on treatment with D_2O), 13.05 ppm (br s, 1H, disappeared on treatment with D_2O). IR: ν 1637, 3220, 3289 cm^{-1}. Anal. Calcd. for $C_{26}H_{25}ClN_2O_3S$: C, 64.92%; H, 5.24%, N, 5.82%; Cl, 7.37%; S, 6.67%. Found: C, 64.78%; H, 5.19%, N, 5.69%; Cl, 7.12%; S, 6.40%.

Table 4
Anti-HIV-1 activity of compounds **4**–**12**, **14**–**18** and **21**–**23** against the WT RT and mutant RTs carrying single amino acid substitutions[a].

Compd	IC_{50} (nM)[b]			
	WT	K103N	Y181I[c]	L100I
4	50	>20,000	>20,000	nd[d]
5	3.7	>20,000	>20,000	nd
6	57	7500	>20,000	nd
7	180	100	>20,000	70
8	70	160	>20,000	40
9	26	24	>20,000	30
10	23	23	>20,000	nd
11	50	218	>20,000	nd
12	7.7	34	201	nd
14	40	540	>20,000	90
16	7000	>20,000	>20,000	5900
16	131	3140	>20,000	270
17	83	5940	>20,000	10
18	89	60	>20,000	960
21	288	12,400	>20,000	200
22	190	>20,000	>20,000	1300
23	2000	>20,000	>20,000	16,250
NVP	400	7000	>20,000	9000
EFV	80	>20,000	400	nd
ETV	10	20	164	12

[a] Data represent mean values of at least three separate experiments.
[b] Compound concentration (IC_{50}, nM) required to inhibit by 50% the RT activity of the indicated strain.
[c] The recombinant HIV-1 RT carrying the Y181I mutation was comparable to the Y181C substitution in terms of drug resistance, from an enzymological point of view [17].
[d] Data of D,L racemic mixture.

Table 5
Anti-HIV-1 activity of racemate **14** and its enantiomers **24** and **25** against the WT RT and mutant RTs carrying single amino acid substitutions.[a]

Compd (*Chirality*)	IC_{50} (nM)[b]				
	WT	K103N	Y181I or Y181C[c]	L100I	V106A
14[d] (*R,S*)	40	540	8228[c]	70	50
24 (*R*)	39	90	2531[c]	50	65
25 (*S*)	50	9400	>20000[c]	80	28
NVP	400	7000	>20,000	9000	nd
EFV	80	>20,000	400	120	nd
ETV	10	20	164	12	10

[a] Data represent mean values of at least three separate experiments.
[b] Compound concentration (IC_{50}, nM) required to inhibit by 50% the RT activity of the indicated strain.
[c] The recombinant HIV-1 RT carrying the Y181I mutation was comparable to the Y181C substitution in terms of drug resistance, from an enzymological point of view [17].
[d] Data of D,L racemic mixture.

*5.1.12. 5-Chloro-N-(2-chlorophenethyl)-3-((3,5-dimethylphenyl) sulfonyl)-1H-indole-2-carboxamide (**16**)*

It was synthesized as **4** starting from **26** and 2-(2-chlorophenyl) ethanamine. Yield 33%, mp 217 °C (from aqueous DMF). ^{1}H NMR (DMSO-d_6): δ 2.31 (s, 6H), 3.01–3.09 (m, 2H), 3.57–3.64 (m, 2H), 7.27–7.37 (m, 4H), 7.44–7.56 (m, 3H), 7.63 (s, 2H), 7.95 (d, J = 3.6 Hz, 1H), 9.17 (t, J = 4.7 Hz, 1H, disappeared on treatment with D_2O), 13.08 ppm (br s, 1H, disappeared on treatment with D_2O). IR: ν 1639, 3211, 3271 cm^{-1}. Anal. Calcd. for $C_{25}H_{22}Cl_2N_2O_3S$: C, 59.88%; H, 4.42%, N, 5.59%; Cl, 14.14%; S, 6.39%. Found: C, 59.70%; H, 4.36%, N, 5.44%; Cl, 13.88%; S, 6.23%.

*5.1.13. 5-Chloro-N-(3-chlorophenethyl)-3-((3,5-dimethylphenyl) sulfonyl)-1H-indole-2-carboxamide (**17**)*

It was synthesized as **4** starting from **26** and 2-(3-chlorophenyl) ethanamine. Yield 25%, mp 212 °C (from aqueous DMF). ^{1}H NMR (DMSO-d_6): δ 2.30 (s, 6H), 2.89–2.99 (m, 2H), 3.57–3.64 (m, 2H), 7.26–7.37 (m, 5H), 7.42 (s, 1H), 7.52–7.61 (m, 3H), 7.92 (s, 1H), 9.12 (t, J = 11.5 Hz, 1H, disappeared on treatment with D_2O), 13.04 ppm (br s, 1H, disappeared on treatment with D_2O). IR: ν 1646, 3190, 3292 cm^{-1}. Anal. Calcd. for $C_{25}H_{22}Cl_2N_2O_3S$: C, 59.88%; H, 4.42%, N, 5.59%; Cl, 14.14%; S, 6.39%. Found: C, 59.64%; H, 4.39%, N, 5.44%; Cl, 13.96%; S, 6.22%.

*5.1.14. 5-Chloro-N-(4-chlorophenethyl)-3-((3,5-dimethylphenyl) sulfonyl)-1H-indole-2-carboxamide (**18**)*

It was synthesized as **4** starting from **26** and 2-(4-chlorophenyl) ethanamine. Yield 80%, mp 220–225 °C (from ethanol). ^{1}H NMR (DMSO-d_6): δ 2.30 (s, 6H), 2.87–2.94 (m, 2H), 3.55–3.64 (m, 2H), 7.25–7.35 (m, 6H), 7.51–7.61 (m, 3H), 7.93 (d, J = 2.0 Hz, 1H), 9.08 (br s, 1H, disappeared on treatment with D_2O), 13.05 ppm (br s, 1H, disappeared on treatment with D_2O). IR: ν 1649, 3197, 3286 cm^{-1}. Anal. Calcd. for $C_{25}H_{22}Cl_2N_2O_3S$: C, 59.88%; H, 4.42%, N, 5.59%; Cl, 14.14%; S, 6.39%. Found: C, 59.71%; H, 4.40%, N, 5.40%; Cl, 13.84%; S, 6.12%.

*5.1.15. 5-Chloro-3-((3,5-dimethylphenyl)sulfonyl)-N-(1-phenylpropan-2-yl)-1H-indole-2-carboxamide (**19**)*

It was synthesized as **4** starting from **26** and 1-phenylpropan-2-amine. Yield 33%, mp 214–216 °C (from ethanol). ^{1}H NMR ($CDCl_3$): δ 1.36 (d, J = 6.5 Hz, 3H), 2.33 (s, 6H), 2.83–2.88 (m, 1H), 3.04–3.09 (m, 1H), 4.45–4.52 (m, 1H), 7.17 (s, 1H), 7.21–7.24 (m, 1H), 7.28–7.34 (m, 5H), 7.38–7.40 (m, 1H), 7.48 (s, 2H), 8.21 (s, 1H), 9.63 (d, J = 8.4 Hz, 1H, disappeared on treatment with D_2O), 10.32 ppm (br s, 1H, disappeared on treatment with D_2O). IR: ν 1642, 3233 cm^{-1}. Anal. Calcd. for $C_{26}H_{25}ClN_2O_3S$: C, 64.92%; H, 5.24%, N, 5.82%; Cl, 7.37%; S, 6.67%. Found: C, 64.81%; H, 5.15%, N, 5.66%; Cl, 7.20%; S, 6.54%.

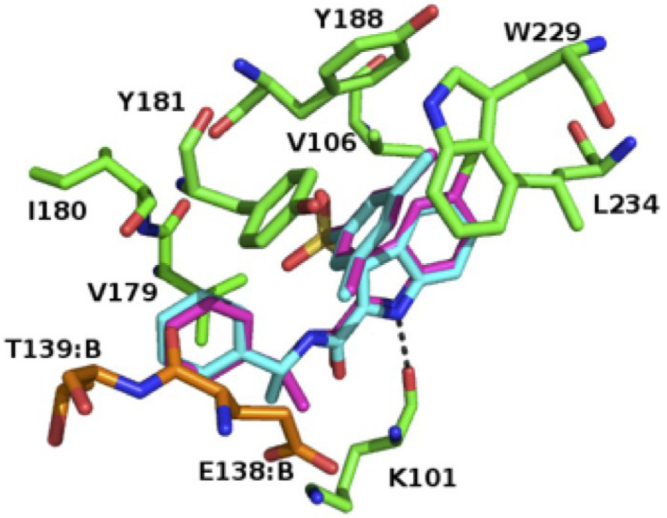

Fig. 1. Binding mode of derivatives **24** (cyan) and **25** (magenta) into the NNBS of the WT RT. Residues involved in the binding are reported as stick. Residues of B chain are reported in orange stick. (For interpretation of the references to colour in this figure legend, the reader is referred to the web version of this article.)

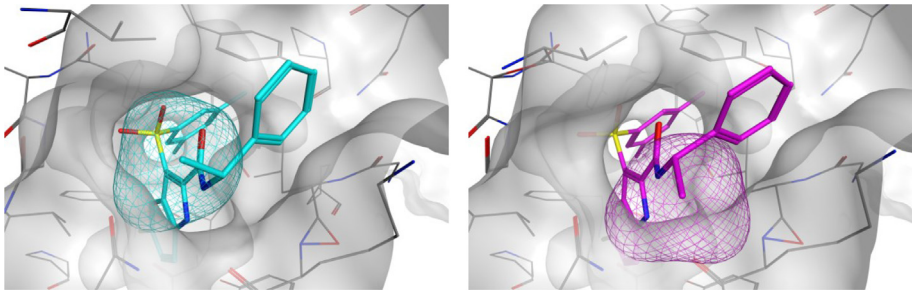

Fig. 2. Binding mode of derivatives **24** (cyan) and **25** (magenta) into the NNBS of the K103N RT. The surface (gray) representation clearly shows that the methyl group of **24** well closes the entrance channel, while for **25** the methyl group points to the bottom of the cleft. (For interpretation of the references to colour in this figure legend, the reader is referred to the web version of this article.)

*5.1.16. 5-Chloro-3-((3,5-dimethylphenyl)sulfonyl)-N-(2-phenylpropyl)-1H-indole-2-carboxamide (**20**)*

It was synthesized as **4** starting from **26** and 2-phenylpropan-1-amine. Yield 33%, mp 209–212 °C (from ethanol). ^{1}H NMR (DMSO-d_6): δ 1.31 (d, J = 6.7 Hz, 3H), 2.30 (s, 6H), 3.04–3.09 (m, 1H), 3.53 (t, J = 5.9 Hz, 2H), 7.22–7.32 (m, 7H), 7.52 (d, J = 9.0 Hz, 1H), 7.57 (s, 2H), 7.90 (s, 1H), 9.07 (t, J = 5.1 Hz, 1H, disappeared on treatment with D_2O), 12.98 ppm (br s, 1H, disappeared on treatment with D_2O). IR: ν 1641, 3230 cm^{-1}. Anal. Calcd. for $C_{26}H_{25}ClN_2O_3S$: C, 64.92%; H, 5.24%, N, 5.82%; Cl, 7.37%; S, 6.67%. Found: C, 64.72%; H, 5.19%, N, 5.68%; Cl, 7.21%; S, 6.49%.

*5.1.17. 5-Chloro-3-((3,5-dimethylphenyl)sulfonyl)-N-(2-methylphenethyl)-1H-indole-2-carboxamide (**21**)*

It was synthesized as **4** starting from **26** and 2-(2-tolyl)ethanamine. Yield 25%, mp 214–216 °C (from ethanol). ^{1}H NMR (DMSO-d_6): δ 2.31 (s, 6H), 2.36 (s, 3H), 2.88–2.95 (m, 2H), 3.47–3.59 (m, 2H), 7.11–7.17 (m, 3H), 7.24–7.27 (m, 2H), 7.32–7.38 (m, 1H), 7.52–7.56 (m, 1H), 7.63 (s, 2H), 7.95 (d, J = 2.1 Hz, 1H), 9.14 (br s, 1H, disappeared on treatment with D_2O), 13.03 ppm (br s, 1H, disappeared on treatment with D_2O). IR: ν 1651, 3226, 3282 cm^{-1}. Anal. Calcd. for $C_{26}H_{25}ClN_2O_3S$: C, 64.92%; H, 5.24%, N, 5.82%; Cl, 7.37%; S, 6.67%. Found: C, 64.77%; H, 5.21%, N, 5.68%; Cl, 7.09%; S, 6.44%.

*5.1.18. 5-Chloro-3-((3,5-dimethylphenyl)sulfonyl)-N-(3-methylphenethyl)-1H-indole-2-carboxamide (**22**)*

It was synthesized as **4** starting from **26** and 2-(3-tolyl)ethanamine. Yield 31%, mp 202–204 °C (from ethanol). ^{1}H NMR (DMSO-d_6): δ 2.27 (s, 3H), 2.30 (s, 6H), 2.87 (t, J = 7.0 Hz, 2H), 3.55–3.59 (m, 2H), 7.03 (d, J = 7.8 Hz, 1H), 7.09–7.19 (m, 3H), 7.26 (s, 1H), 7.33 (d, J = 8.6 Hz, 1H), 7.52 (d, J = 8.7 Hz, 1H), 7.60 (s, 2H), 7.92 (s, 1H), 9.08 (br s, 1H, disappeared on treatment with D_2O), 13.01 ppm (br s, 1H, disappeared on treatment with D_2O). IR: ν 1648, 3211, 3289 cm^{-1}. Anal. Calcd. for $C_{26}H_{25}ClN_2O_3S$: C, 64.92%; H, 5.24%, N, 5.82%; Cl, 7.37%; S, 6.67%. Found: C, 64.70%; H, 5.16%, N, 5.59%; Cl, 7.20%; S, 6.45%.

*5.1.19. 5-Chloro-3-((3,5-dimethylphenyl)sulfonyl)-N-(4-methylphenethyl)-1H-indole-2-carboxamide (**23**)*

It was synthesized as **4** starting from **26** and 2-(4-tolyl)ethanamine. Yield 43%, mp 206–207 °C (from ethanol). ^{1}H NMR (DMSO-d_6): δ 2.26 (s, 3H), 2.30 (s, 6H), 2.84–2.87 (m, 2H), 3.52–3.58 (m, 2H), 7.11 (d, J = 6.8 Hz, 2H), 7.20 (d, J = 7.4 Hz, 2H), 7.26 (s, 1H), 7.33 (d, J = 7.9 Hz, 1H), 7.52 (d, J = 8.5 Hz, 1H), 7.60 (s, 2H), 7.92 (s, 1H) 9.08 (br s, 1H, disappeared on treatment with D_2O), 13.02 ppm (br s, 1H, disappeared on treatment with D_2O). IR: ν 1642, 3208, 3299 cm^{-1}. Anal. Calcd. for $C_{26}H_{25}ClN_2O_3S$: C, 64.92%; H, 5.24%, N, 5.82%; Cl, 7.37%; S, 6.67%. Found: C, 64.80%; H, 5.19%, N, 5.70%; Cl, 7.20%; S, 6.44%.

*5.1.20. N-(4-Aminobenzyl)-5-chloro-3-((3,5-dimethylphenyl) sulfonyl)-1H-indole-2-carboxamide (**12**)*

To a solution of **11** (100 mg, 0.24 mmol) in ethyl acetate (14 mL) was added tin(II) chloride dihydrate (160 mg, 0.72 mmol), and the reaction mixture was heated at reflux for 3 h. After cooling, the reaction mixture was adjusted to pH 8 with a saturated solution of sodium hydrogencarbonate, filtered and extracted with ethyl acetate. Organic layer was dried and filtered. Removal of the solvent gave a residue that was purified by column chromatography (silica gel, ethyl acetate:*n*-hexane = 7:3 as eluent) to furnish **12** (10 mg, 9%), mp 185 °C dec (from ethanol). ^{1}H NMR (DMSO-d_6): δ 2.26 (s, 6H), 4.38 (s, 2H), 5.03 (s, 2H, disappeared on treatment with D_2O), 6.52–6.56 (m, 2H), 7.06–7.10 (m, 2H), 7.23–7.25 (m, 1H), 7.31–7.36 (m, 1H), 7.50–7.61 (m, 3H), 7.93–7.95 (m, 1H), 9.26 (br s, 1H, disappeared on treatment with D_2O), 13.03 ppm (br s, 1H, disappeared on treatment with D_2O). IR: ν 1667, 2980, 3225 cm^{-1}. Anal. Calcd. for $C_{24}H_{22}ClN_3O_3S$: C, 61.60%; H, 4.74%, N, 8.98%; Cl, 7.58%; S, 6.85%. Found: C, 61.37%; H, 4.68%, N, 8.74%; Cl, 7.39%; S, 6.61%.

*5.1.21. tert-Butyl 4-nitrobenzylcarbamate (**28**)*

A mixture of (4-nitrophenyl)methanamine hydrochloride (500 mg, 2.65 mmol) and di-*tert*-butyl dicarbonate (634 mg, 2.91 mmol) in anhydrous dichloromethane (10.8 mL) was cooled to 0 °C in ice-water bath. Triethylamine (691 mg, 0.96 mL, 6.39 mmol) was added dropwise and the resulting mixture was stirred at room temperature for 2 h. The reaction mixture was diluted with water and extracted with dichlorometane. The organic layer was washed with brine, dried and filtered. Removal of the solvent gave compound **28** (610 mg, 91%) as a slurry. ^{1}H NMR (DMSO-d_6): δ 1.37 (s, 9H), 4.23 (d, J = 5.7 Hz, 2H), 7.46–7.56 (m, 3H), 8.18 ppm (d, J = 8.4 Hz, 2H). IR: ν 1675, 2982, 3350 cm^{-1}.

*5.1.22. tert-Butyl 4-aminobenzylcarbamate (**29**)*

To a mixture of **28** (590 mg, 2.33 mmol) in methanol (20.6 mL) was added Pd/C (62 mg; 10% pp). The reaction mixture was hydrogenated under 35 PSI pressure at room temperature and for 2 h. The reaction mixture was filtered and evaporated. Residue was purified by silica gel column chromatography (ethyl acetate:*n*-hexane = 1:1 as eluent) to furnish **29** (520 mg; 100%) as an oil. ^{1}H NMR (DMSO-d_6): δ 1.37 (s, 9H), 3.91 (d, J = 6.0 Hz, 2H), 4.90 (s, 2H, disappeared on treatment with D_2O), 6.47 (d, J = 8.1 Hz, 2H), 6.87 (d, J = 8.0, 2H), 7.13 ppm (s, 1H, disappeared on treatment with D_2O). IR: ν 1695, 2974 cm^{-1}.

*5.1.23. tert-Butyl (4-dimethylaminophenyl)carbamate (**30**)*

A mixture of **29** (230 mg; 1.03 mmol), anhydrous potassium carbonate (355 mg, 2.6 mmol) and dimethylsulfate (129 mg, 0.1 mL; 1.03 mmol) in anhydrous acetone (25.5 mL) was stirred at room temperature for 16 h. The reaction mixture was diluted with water and extracted with ethyl acetate. Organic layer was washed with brine, dried and filtered. Removal of the solvent gave a residue that was purified by flash chromatography (silica gel, ethyl acetate/*n*-hexane as eluent) to furnish **28** (100 mg, 41%) as a slurry. ^{1}H NMR (DMSO-d_6): δ 1.37 (s, 9H), 2.84 (s, 6H), 3.97 (d, J = 5.7 Hz, 2H), 6.65 (d, J = 8.4 Hz, 2H), 7.04 (d, J = 8.2 Hz, 2H), 7.20 ppm (s, 1H, disappeared on treatment with D_2O).

*5.1.24. 4-Dimethylaminophenylmethanamine trifluoroacetate (**31**)*

A mixture of **30** (100 mg, 0.39 mmol), dichloromethane (0.4 mL) and trifluoroacetic acid (0.4 mL) was stirred at room temperature for 30 min. The reaction mixture was diluted with diethyl ether and the solvent was evaporated. The obtained product was used without further purification.

*5.1.25. Separation of racemate **14** into the enantiomers **24** and **25***

5.1.25.1. HPLC. HPLC enantioseparations were performed by using the stainless-steel Chiralcel OD (250 mm × 4.6 mm i.d. and 250 × 10 mm i.d.) (Chiral Technologies Europe, Illkirch, France) columns. All chemicals solvents for HPLC were purchased from Aldrich (Italy) and used without further purification. The analytical HPLC apparatus consisted of a Perkin–Elmer (Norwalk, CT, USA) 200 lc pump equipped with a Rheodyne (Cotati, CA, USA) injector, a 20 μl sample loop, an HPLC Dionex CC-100 oven (Sunnyvale, CA, USA) and a Jasco (Jasco, Tokyo, Japan) Model CD 2095 Plus UV/CD detector. For semipreparative separations a Perkin–Elmer 200 LC pump equipped with a Rheodyne injector, a 1 mL sample loop, a Perkin–Elmer LC 101 oven and Waters 484 detector (Waters Corporation, Milford, MA, USA) were used. The signal was acquired and processed by Clarity software (DataApex, Prague, The Czech Republic).

5.1.25.2. Circular dichroism. The circular dichroism (CD) spectra were measured by using a Jasco Model J-700 spectropolarimeter. The optical path and temperature were set at 0.1 mm and 20 °C, respectively. The spectra are average computed over three instrumental scans and the intensities are presented in terms of ellipticity values (mdeg).

5.2. Biological assays

5.2.1. Inhibition of HIV-induced cytopathicity

Biological activity of the compounds was tested in the lymphoid MT-4 cell line (received from the NIH AIDS Reagent Program) against the WT HIV-1 NL4-3 strain and the different mutant HIV-1 strains, as described before [19]. Briefly, MT-4 cells were infected with the appropriate HIV-1 strain (or mock-infected to determine cytotoxicity) in the presence of different drug concentrations. At day five post-infection, a tetrazolium-based colorimetric method (MTT method) was used to evaluate the number of viable cells. The methodology for the anti-HIV assays in CEM cells had been described previously [20]. Briefly, human CEM cell cultures ($\sim 3 \times 10^5$ cells/mL^{-1}) were infected with $\sim$100 $CCID_{50}$ HIV-1 IIIB or HIV-2 ROD per mL and seeded in 200 μL-well microtiter plates, containing appropriate dilutions of the test compounds. After 4 days of incubation at 37 °C, syncytia cell formation was examined microscopically in the CEM cell cultures.

5.2.2. Enzymatic assay procedures

5.2.2.1. Chemicals. [^{3}H]dTTP (40 Ci/mmol) was from Amersham and unlabeled dNTP's from Boehringer. Whatman was the supplier of the GF/C filters. All other reagents were of analytical grade and purchased from Merck or Fluka. The homopolymer poly(rA) (Pharmacia) was mixed at weight ratios in nucleotides of 10:1, to the oligomer oligo(dT)$_{12-18}$ (Pharmacia) in 20 mM Tris–HCl (pH 8.0), containing 20 mM KCl and 1 mM EDTA, heated at 65 °C for 5 min and then slowly cooled at room temperature. The coexpression vectors pUC12N/p66(His)/p51with the wild-type or the mutant forms of HIV-1 RT p66 were kindly provided by Dr. S. H. Hughes (NCI-Frederick Cancer Research and Development Center). Proteins were expressed in *E. coli* and purified as described [21]. RNA-dependent DNA polymerase activity was assayed as follows: a final volume of 25 μL contained reaction buffer (50 mM Tris–HCl pH 7.5, 1 mM DTT, 0.2 mg/mL BSA, 4% glycerol), 10 mM $MgCl_2$, 0.5 μg of poly(rA)/oligo(dT)$_{10:1}$ (0.3 μM 3′-OH ends), 10 μM [3H]-dTTP (1 Ci/mmol) and 2–4 nM RT. Reactions were incubated at 37 °C for the indicated time. 20 μL-Aliquots were then spotted on glass fiber filters GF/C which were immediately immersed in 5% ice-cold TCA. Filters were washed twice in 5% ice-cold TCA and once in ethanol for 5 min, dried and acid-precipitable radioactivity was quantitated by scintillation counting. Reactions were performed under the conditions described for the HIV-1 RT RNA-dependent DNA polymerase activity assay. Incorporation of radioactive dTTP into poly(rA)/oligo(dT) at different substrate (nucleic acid or dTTP) concentrations was monitored in the presence of increasing fixed amounts of inhibitor. Data were then plotted according to Lineweaver–Burke and Dixon. For K_i determination, an interval of inhibitor concentrations between 0.2 K_i and 5 K_i was used.

5.3. Molecular modeling

All molecular modeling studies were performed on a MacPro dual 2.66 GHz Xeon running Ubuntu 12.04 LTS. The RT structures were downloaded from the PDB (WT RT: 2rf2 [17]; K103N mutated RT: 1fk0 [22]). Hydrogen atoms were added to the protein using Molecular Operating Environment (MOE) 2007.09 [23] and minimized, keeping all the heavy atoms fixed until a rmsd gradient of 0.05 kcal mol^{-1} Å^{-1} was reached. Ligand structures were built with MOE and minimized using the MMFF94× force field until a rmsd gradient of 0.05 kcal mol^{-1} Å^{-1} was reached. The docking simulations were performed using PLANTS 1.1 [24]. The images in the manuscript were generated by using PyMOL 1.2 [25] and MOE softwares.

Acknowledgments

This research project was supported by grant 2012 of Istituto Pasteur-Fondazione Cenci Bolognetti and the Spanish MINECO SAF2010-21617-C02 and BFU 2012-31569. Authors thank Prof. Jan Balzarini, Rega Institute for Medical Research, Katholieke Universiteit Leuven, B-3000 Leuven, Belgium, for the evaluation of some compounds against HIV-1 IIIB and HIV-2 ROD strains.

References

[1] R. Lafemina, Antiviral Research: Strategies in Antiviral Drug Discovery (Chapters 2–7), AMS Press, Washington, 2009.
[2] H.W. Virgin, B.D. Walker, Immunology and the elusive AIDS vaccine, Nature 464 (2011) 224–231.
[3] Antiretroviral Drugs Used in the Treatment of HIV Infection, FDA (last update Dec. 18th, 2012).
[4] J.A. Este, T. Cihlar, Current status and challenges of antiretroviral research and therapy, Antiviral Research 85 (2010) 25–33.

[5] L. Menéndez-Arias, Molecular basis of human immunodeficiency virus type 1 drug resistance: overview and recent developments, Antiviral Research 98 (2013) 93–120.
[6] P.M. Grant, A.R. Zolpa, Optimal antiretroviral therapy: HIV-1 treatment strategies to avoid and overcome drug resistance, Current Opinion in Investigational Drugs 11 (2010) 901–910.
[7] (a) K.J. Cortez, F. Maldarelli, Clinical management of HIV drug resistance, Viruses 3 (2011) 347–378;
(b) T. Howkins, Understanding and managing the adverse effects of antiretroviral therapy, Antiviral Research 85 (2010) 201–209.
[8] V. Famiglini, A. Coluccia, A. Brancale, G. La Regina, R. Silvestri, Arylsulfone-based HIV-1 non-nucleoside reverse transcriptase inhibitors, Future Medicinal Chemistry 18 (2013) 2141–2156.
[9] R. Silvestri, G. De Martino, G. La Regina, M. Artico, S. Massa, L. Vargiu, M. Mura, A.G. Loi, T. Marceddu, P. La Colla, Novel indolyl aryl sulfones active against HIV-1 carrying NNRTI resistance mutations: synthesis and SAR studies, Journal of Medicinal Chemistry 46 (2003) 2482–2493.
[10] R. Silvestri, M. Artico, G. De Martino, G. La Regina, R. Loddo, M. La Colla, P. La Colla, Simple, short peptide derivatives of a sulfonylindolecarboxamide (L-737,126) active in vitro against HIV-1 wild-type and variants carrying non-nucleoside reverse transcriptase inhibitor resistance mutations, Journal of Medicinal Chemistry 47 (2004) 3892–3896.
[11] F. Piscitelli, A. Coluccia, A. Brancale, G. La Regina, A. Sansone, C. Giordano, J. Balzarini, G. Maga, S. Zanoli, A. Samuele, R. Cirilli, R.F. La Torre, A. Lavecchia, E. Novellino, R. Silvestri, Indolylarylsulfones bearing natural and unnatural amino acids. Discovery of potent inhibitors of HIV-1 non-nucleoside wild type and resistant mutant strains reverse transcriptase and Coxsackie B4 virus, Journal of Medicinal Chemistry 52 (2009) 1922–1934.
[12] R. Ragno, M. Artico, G. De Martino, G. La Regina, A. Coluccia, A. Di Pasquali, R. Silvestri, Docking and 3-D QSAR studies on indolyl aryl sulfones (IASs). Binding mode exploration at the HIV-1 reverse transcriptase non-nucleoside binding site and design of highly active *N*-(2-hydroxyethyl)carboxyamide and *N*-(2-hydroxyethyl)-carboxyhydrazide derivatives, Journal of Medicinal Chemistry 48 (2005) 213–223.
[13] R. Ragno, A. Coluccia, G. La Regina, G. De Martino, F. Piscitelli, A. Lavecchia, E. Novellino, A. Bergamini, C. Ciaprini, A. Sinistro, G. Maga, E. Crespan, M. Artico, R. Silvestri, Design, molecular modeling, synthesis and anti-HIV-1 activity of new indolyl aryl sulfones. Novel derivatives of the indole-2-carboxamide, Journal of Medicinal Chemistry 49 (2006) 3172–3184.
[14] (a) G. La Regina, A. Coluccia, R. Silvestri, Looking for an active conformation of the future HIV-1 non-nucleoside reverse transcriptase inhibitors, Antiviral Chemistry and Chemotherapy 20 (2010) 231–237;
(b) P. Chong, P. Sebahar, M. Youngman, D. Garrido, H. Zhang, E.L. Stewart, R.T. Nolte, L. Wang, R.G. Ferris, M. Edelstein, K. Weaver, A. Mathis, A. Peat, Rational design of potent non-nucleoside inhibitors of HIV-1 reverse transcriptase, Journal of Medicinal Chemistry 55 (2012) 10601–10609.
[15] G. La Regina, A. Coluccia, A. Brancale, F. Piscitelli, V. Gatti, G. Maga, A. Samuele, C. Pannecouque, D. Schols, J. Balzarini, E. Novellino, R. Silvestri, Indolylarylsulfones as HIV-1 non-nucleoside reverse transcriptase inhibitors. New cyclic substituents at the indole-2-carboxamide, Journal of Medicinal Chemistry 54 (2011) 1587–1598.
[16] J.W. Corbett, J.D. Rodgers, Discovery of second generation of quinazoline non-nucleoside reverse transcriptase inhibitors of HIV-1, Progress in Medicinal Chemistry 40 (2002) 63–105.
[17] Z. Zhao, S.E. Wolkenberg, M. Lu, V. Munshi, G. Moyer, M. Feng, A.V. Carella, L.T. Ecto, L.J. Gabryelski, M.T. Lai, S.G. Prasad, Y. Yan, G.B. McGaughey, M.D. Miller, C.W. Lindsley, G.D. Hartman, J.P. Vacca, T.M. Williams, Novel indole-3-sulfonamides as potent HIV non-nucleoside reverse transcriptase inhibitors (NNRTIs), Bioorganic & Medicinal Chemistry Letters 18 (2008) 554–559.
[18] M. Geitmann, T. Unge, H.U. Danielson, Interaction kinetic characterization of HIV-1 reverse transcriptase non-nucleoside inhibitor resistance, Journal of Medicinal Chemistry 49 (2006) 2375–2387.
[19] E. Gonzalez-Ortega, E. Ballana, R. Badia, B. Clotet, J.A. Estè, Compensatory mutations rescue the virus replicative capacity of VIRIP-resistant HIV-1, Antiviral Research 92 (2011) 479–483.
[20] A.N. Van Nhien, C. Tomassi, C. Len, J.L. Marco-Contelles, J. Balzarini, C. Pannecouque, E. De Clercq, D. Postel, First synthesis and evaluation of the inhibitory effects of aza analogues of TSAO on HIV-1 replication, Journal of Medicinal Chemistry 48 (2005) 4276–4284.
[21] G. Maga, M. Amacker, N. Ruel, U. Hubsher, S. Spadari, Resistance to nevirapine of HIV-1 reverse transcriptase mutants: loss of stabilizing interactions and thermodynamic or stearic barriers are induced by different single amino acid substitutions, Journal of Molecular Biology 274 (1997) 738–747.
[22] J. Ren, J. Milton, K.L. Weaver, S.A. Short, D.I. Stuart, D.K. Stammers, Structural basis for the resilience of efavirenz (DMP-266) to drug resistance mutations in HIV-1 reverse transcriptase, Structure Folding and Design 8 (2000) 1089–1094.
[23] Molecular Operating Environment (MOE). Chemical Computing Group, Inc. Montreal, Quebec, Canada. www.chemcomp.com.
[24] O. Korb, T. Stutzle, T.E. Exner, PLANTS: application of ant colony optimization to structure-based drug design, in: M. Dorigo, L.M. Gambardella, M. Birattari, A. Martinoli, R. Poli, T. Stutzle (Eds.), In Ant Colony Optimization and Swarm Intelligence, Proceedings of the 5th International Workshop, ANTS, Lecture Notes in Computer Science, Series 4150, Springer, Berlin, 2006, pp. 247–258.
[25] PyMOL version 1.2r1; DeLano Scientific LLC: San Carlos, CA http://www.pymol.org/.